A MORPHOLOGICAL RECONSTRUCTION ALGORITHM FOR SEPARATING OFF-TERRAIN POINTS FROM TERRAIN POINTS IN LASER SCANNING DATA

H. Arefi, M. Hahn

Dept. of Geomatics, Computer Science and Mathematics, Stuttgart University of Applied Sciences, Stuttgart, Germany
(Hossein.Arefi, Michael.Hahn)@hft-stuttgart.de

KEY WORDS: LIDAR, morphological reconstruction, terrain points, off-terrain points, DTM

ABSTRACT:

During the last decade various techniques have been proposed to extract the ground surface from airborne LIDAR data. The basic problem is the separation of terrain points from off-terrain points which are both recorded by the LIDAR sensor. In particular geometry driven filtering, detection or classification procedures are developed which use knowledge to find points, e.g. on buildings or vegetation. Depending on the application the off-terrain points are excluded from further processing, e.g. for DTM generation, or used, e.g. for building reconstruction.
In this paper a new method is proposed to separate 3D off-terrain points from the terrain points. Morphological grayscale reconstruction plays the key role in the proposed algorithm to produce the bare ground. After a short description of morphological reconstruction an algorithm based on this technique is presented. Issues of the implementation of the morphological reconstruction algorithm are discussed and illustrated. Experiments are carried out with different LIDAR data sets, which point out the capacity of the process.

1. INTRODUCTION

Airborne laser scanning data has become an accepted data source for highly automated acquisition of digital surface models (DSM) as well as for the generation of digital terrain models (DTM). To generate a high quality DTM using LIDAR data, 3D off-terrain points have to be separated from terrain points. Various techniques and filtering methods have been proposed to generate DTM from LIDAR data or other DSMs even though the there is still ongoing research in this field.
In an early work Kilian et al. (Kilian, Haala & Englich, 1996) presented some first ideas to generate a DTM from LIDAR data recorded in wooded areas. Basis of the idea is a morphological opening operation. The lowest points within a given window size is first detected after an opening is first performed on the data set. Then the points in this window that fall within a band above the lowest elevation are considered as ground points and a weighted surface interpolation using those points is applied to compute the DTM. A conclusion of this work was that the size of the structural element used for the opening is a critical parameter for which there is no single optimal value. Therefore, the use of multiple openings with different sizes of structural elements was suggested.
Kraus and Pfeifer (Kraus & Pfeifer, 1998) introduced another algorithm for DTM generation in wooded areas based on linear prediction. They also start with an approximation of the ground surface. The distances from the ground surface to the measured points are used to define weights which in turn are employed in computing the DTM based on the linear prediction model. If the height residual within surface interpolation is above a certain threshold, the corresponding point is classified as an off-terrain point and eliminated from surface interpolation.
Axelsson (Axelsson, 1999) described a method for DTM generation based on progressive densification of a triangular irregular network (TIN). The idea is to connect a surface from below to the point cloud. In every iteration the surface is allowed to fluctuate within certain values and points from the point cloud are added to the TIN. These iterations proceed until no further low ground points can be added any more. The approach has been implemented in the TerraScan software package (TerraScan, 2005).
Vosselman (Vosselman, 2000) proposed a slope based filtering method for separating off-terrain points from terrain points. A point is classified as a terrain point if there is no other point locally around such that the height difference between theses points is larger than an allowed maximum height difference.
Wack and Wimmer (Wack & Wimmer, 2002) proposed a hierarchical grid-based approach for generation of DTMs from airborne laser data. They start with a coarse grid of 9 m grid width and define the raster height by selecting the lowest height from 99% of all points within the raster element. The Laplacian of Gaussian operator in combination with a weight function is utilized to detect and remove the points that are not considered to be ground points.
A progressive morphological filtering method is developed by Zhang et al. (Zhang et al. 2003) with the focus to remove the non-ground measurements from LIDAR datasets. The algorithm utilizes the classical morphological opening and gradually increases the size of the structuring element. The resulting elevation differences are used to classify ground and non-ground points by applying a threshold which depends on the structuring element size.

In the following a filtering approach for detecting and removing the 3D off-terrain points is presented based on a geodesic distance operator (Lantuejoul & Maisonneuve, 1984). Classical morphological operations such as erosion and dilation filter an input image with a specific selectable structuring element. The approach taken with geodesic operators is to consider two input images. An elementary morphological operator is applied to the first image and it is then forced to remain either higher or lower than the second image. In this process any discussion on proper

structuring element sizes becomes superfluous. The overall goal of the morphological reconstruction algorithm presented in the next section is to separate off-terrain points from terrain points. To simplify the algorithmic development the LIDAR data are regularized by generating a regularly spaced elevation grid.
The paper is organized as follows. In Section 2 a brief introduction into morphological reconstruction based on geodesic dilation is given. Section 3 shows an example which contracts the reconstruction approach with classical morphological filtering. Section 4 presents the overall approach for separating terrain and off-terrain points. Experimental investigations are discussed in Section 5 and some conclusions are drawn in the final section.

2. MORPHOLOGICAL RECONSTRUCTION BASED ON GEODESIC DILATION

Morphological grayscale reconstruction based on geodesic dilation employs two input images. These two images are called marker and mask images. Both images must have the same size and the mask image must have intensity values greater or equal to the marker image. In geodesic dilation the marker image is dilated by an elementary isotropic structuring element and the resulting image is forced to remain below the mask image. This means, the mask image acts as a limit for the dilated marker image. In the following the marker image is denoted by J and the mask image by I. Both images are identical in size, and $J \le I$.

The classical grayscale dilation of J with structuring element B is given by

$$\delta(J) = J \oplus B \qquad (1)$$

The symbol $\oplus$ is used for the dilation operation. The geodesic dilation of size 1 of the marker image J with respect to mask image I is defined as:

$$\delta_I^{(1)}(J) = (J \oplus B) \wedge I, \qquad (2)$$

In this equation, $\wedge$ stands for the point-wise minimum between the dilated marker image and the mask image, $J \oplus B$ is the dilation of J with the elementary isotropic structuring element B. The geodesic dilation of size n of the marker image J with respect to a mask image I is obtained by performing n successive geodesic dilation of size 1 of J with respect to I

$$\delta_I^{(n)}(J) = \underbrace{\delta_I^{(1)}(J) \circ \delta_I^{(1)}(J) \circ \cdots \circ \delta_I^{(1)}(J)}_{n \text{ times}}. \qquad (3)$$

Equation 3 defines the morphological reconstruction by geodesic dilation of the mask I from marker the J. The desired reconstruction is achieved by carrying out geodesic dilations until stability is reached (Vincent, 1993). In other words, morphological reconstruction can be thought of conceptually as repeated dilations of the marker image until the contour of the marker image fits under the mask image. In this way, the peaks in the marker image spread out, or dilate. Each successive dilation operation is forced to lie underneath the mask. When further dilations do not change the marker image any more, the processing is finished. The final dilation creates the reconstructed image. Figure 1 illustrates the morphological reconstruction by means of geodesic dilations of a 1D signal I from a marker signal $J = I - h$.

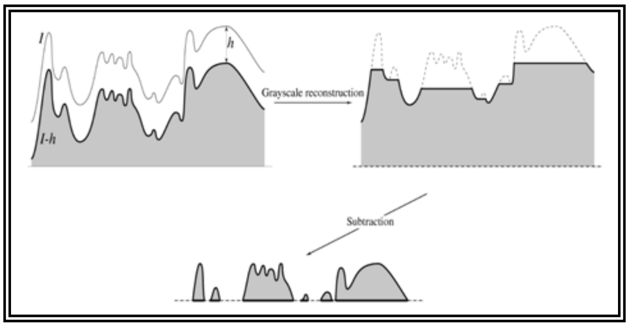

Figure 1. Morphological reconstruction by geodesic dilation of a 1D mask signal I from a marker signal $J = I - h$. The mask signal and the marker signal produced by arithmetic subtraction of the constant offset from the mask are depicted in the upper-left part of the figure. The result of grayscale reconstruction using geodesic dilation is shown in the upper-right part. The subtraction of the reconstructed signal from the mask signal is plotted in the row below (Courtesy of Vincent, 1993).

3. GEODESIC MORPHOLOGY VERSUS CLASSICAL MORPHOLGY

One possibility to compare the results of morphological grayscale reconstruction based on geodesic dilation and with the results of a classical opening is to look at the subtraction result which is shown in Figure 1 for morphological reconstruction. The subtraction result between an image and a grayscale opening of this image is commonly called TopHat filtered image.
Applied to surfaces instead of images the term normalized digital surface model (nDSM) is often used instead of TopHat filtered DSM (Weidner, 1997, Ameri, 2000). In the following we will stick to the term nDSM.

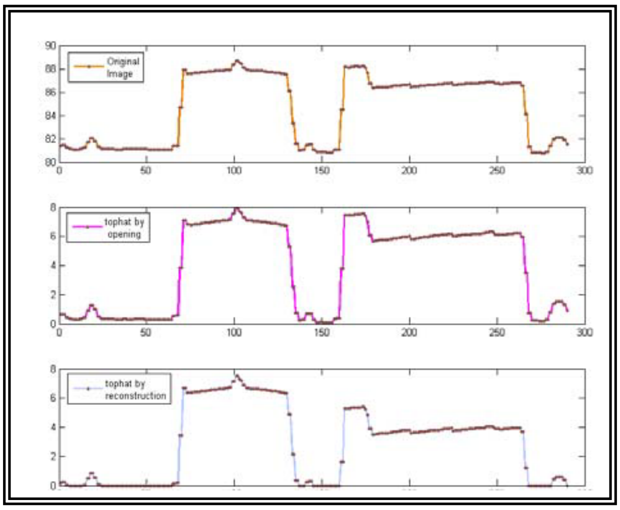

Figure 2. Comparison of an nDSM produced by TopHat filtering (middle) and grayscale reconstruction (below). The input profile taken from the LIDAR range image is shown above.

A comparison of both concepts is illustrated in Figure 2. A profile is taken from the LIDAR data used in the experimental investigations (Section 5).
In this example the size of the structuring element of the TopHat filter was 100 by 100 pixels which correspond to 100 meters by 100 meters. Defining the structuring element size is one of the critical aspects of morphological filtering. Either the structuring element should be defined by using knowledge about the shape, size, and orientation of the structures, which have to be filtered or approaches based on a variety of structuring element sizes have to be developed (Arefi & Hahn, 2005), which eases the dependency on the proper selection of filter kernel sizes.
If the TopHat filtered DSM is used for the separation of terrain points from non-terrain points often elevation difference thresholds are applied to the nDSM. The elevation difference thresholds may be determined by taking slope into account but it remains a crucial aspect to select a (or several) proper thresholds.
The big advantage of the filtering approach based on morphological reconstruction is that geodesic dilation just employs the elementary isotropic structuring element. Thus there is no need to select structuring element sizes. The successively applied geodesic dilations of size 1 run automatically until stability is reached. Further, Figure 2 indicates that the morphological opening tends to produce a surface that lies below the terrain points so that the Tophat filtered DSM is rarely at the zero level. Opposed to that the resulting nDSM found by the reconstruction approach is often at the zero level for the terrain points thus separates off-terrain points from terrain points almost naturally. The nDSM points with values greater then zero may have to be further classified taking terrain slope or other features into account.

4. SEPARATING TERRAIN AND OFF-TERRAIN BASED ON MORPHOLOGICAL RECONSTRUCTION

The algorithm for separating off-terrain points from terrain points in a LIDAR image based on geodesic morphological reconstruction is outlined in Figure 3. The starting point for the proposed algorithm is the regularly spaced elevation grid points found by nearest neighbor interpolation of the raw 3D points. The nearest neighbor interpolation is used to avoid smoothing over discontinuities given in the raw data.

The input to the process is the mask image. If LIDAR first and last pulse range data are given mostly the last pulse image is used. In the first step a marker image is generated with respect to the mask image. In general, an appropriate marker image is determined using knowledge about the expected result and known facts about the image or the physics of the object it represents (Jähne et al., 1999). Most commonly a marker image is generated by subtracting a constant value from the mask image as illustrated in Figure 1. To avoid problems caused by an improperly selected offset we propose to use a sequence of constant offset values to create a sequence of marker images. Formally this is obtained by

$$\begin{aligned} J &= I - h \\ h &= i \text{ to } j \end{aligned} \qquad (4)$$

The next step is to calculate the geodesic dilation of size 1 of the marker image with respect to the mask image. According to Equation 3 this process will be continued until the pixel values do not change any more by a further geodesic dilation of the marker image. The result of the successively performed geodesic dilations is the morphologically reconstructed image.

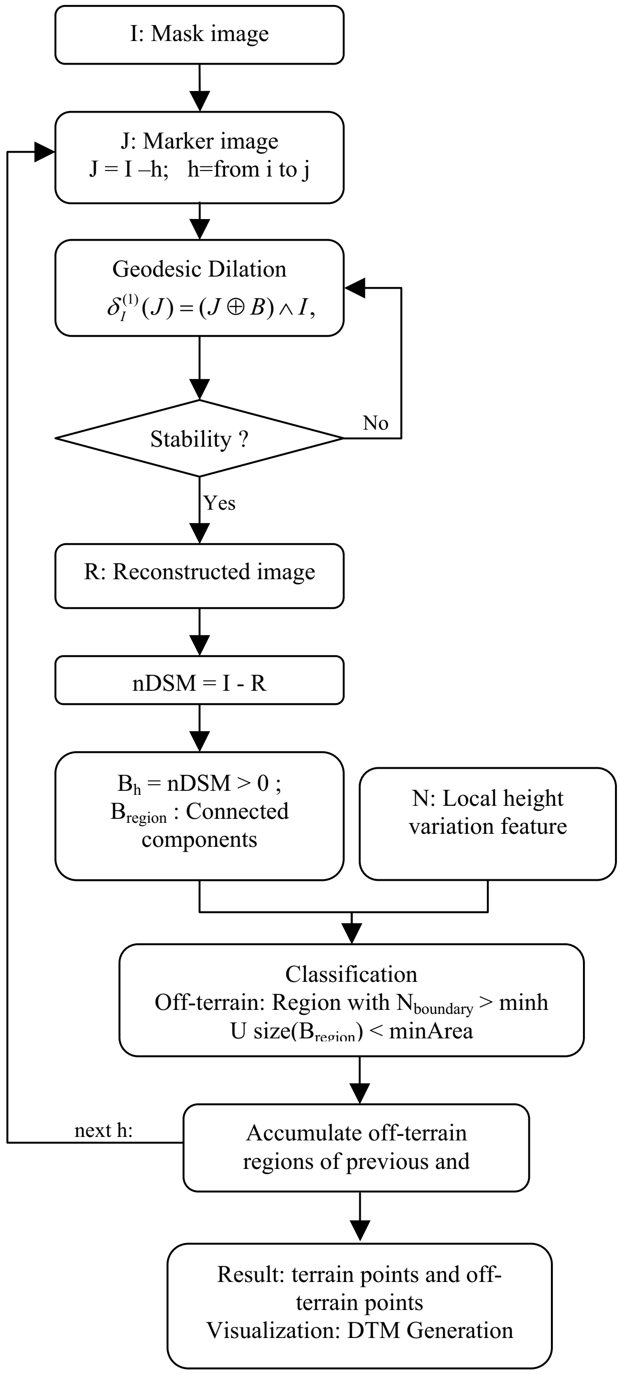

Figure 3. Proposed algorithm for separating terrain and off-terrain points and regions from airborne LIDAR data

By subtracting the reconstructed image from the mask image the normalized DSM (nDSM) is obtained. .
A first classification of terrain and off-terrain points is carried out by binarising the nDSM. Any point (in the nDSM) above zero is collected as an off-terrain point. Off-terrain regions are

formed by calculating connected components of the off-terrain points.

For further analysis features are determined for each off-terrain region. Conceptually ideal would be to extract features which are best suited for making the decision on whether a regions is an off-terrain region or not. In this work we focus on the size of the region and the local height difference along the boundary of the region. By subtracting maximum and minimum values in local 3 by 3 windows moved over the mask image along the region boundary the local height differences are found. The average local height difference is calculated and used as the second feature. Classification is now using these two features. Very small regions as well as single points in the nDSM are classified as off-terrain points basically due to the outlier behavior of these points. All other regions which show up with a certain elevation difference along the boundary are also classified as off-terrain regions. For the remaining regions the discontinuity (or slope) along the boundary is not significant thus they are considered to be terrain regions.
More specific knowledge could be used to classify the regions more specifically into vehicles, buildings, trees, etc., but this is beyond the scope of our current work.

These steps from creating the marker image to the classification of the off-terrain regions will be repeated for all marker images produced with different height offset (h) values. The classification takes the results of previous iterations into account by merging it with the classified off-terrain regions of the current iteration. At the end of the process the classification result represents two classes: off-terrain regions and terrain regions.

For visualizing the impact of separating terrain and off-terrain points on the surface model all off-terrain points are removed from the original LIDAR data. A new interpolation is calculated using the terrain points as input which basically produces a Digital Terrain Model.

One aspect of the proposed algorithm for separating terrain and off-terrain regions should be discussed in some more detail.

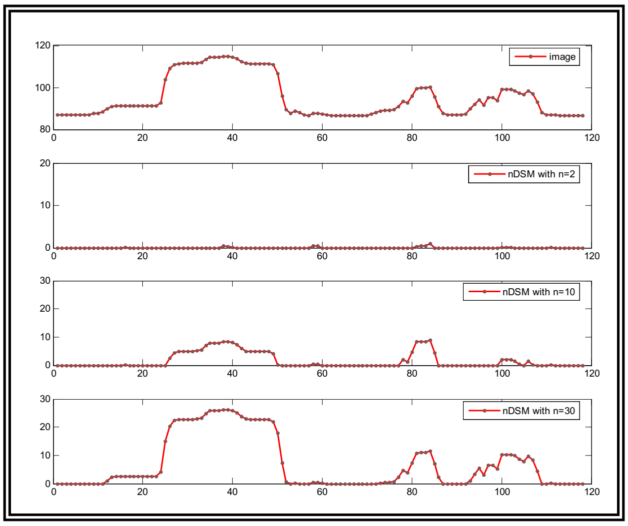

Figure 4. Different nDSMs based on grayscale reconstruction. From top to bottom: mask image, nDSM with marker I-2, nDSM with marker I-10, and nDSM with marker I-30

As already mentioned a sequence of marker images is used rather than just one marker image. The impact of taking different height offsets into account in creating marker images is shown in Figure 4. With small height offsets the low height off-terrain regions are addressed only. Figure 5 shows that some of these regions are representing only a part, mostly the top, of larger regions. By increasing the height offset the high off-terrain regions are taken into account. Not necessarily are the high off-terrain regions also the bigger ones. But in contrast to the TopHat filtering approaches, which filter the data with different kernel sizes to cope with objects of different size, the extent of an object is no factor which has to be taken into account in our approach

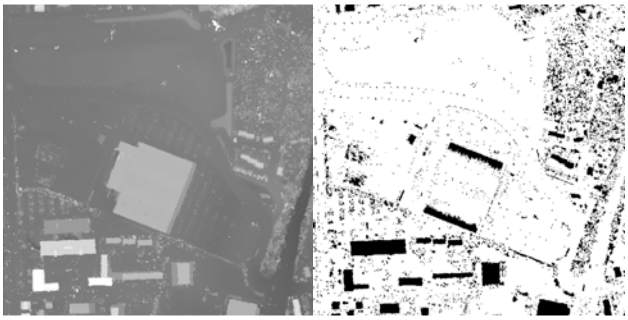

(a) Mask image (b) nDSM , h=5

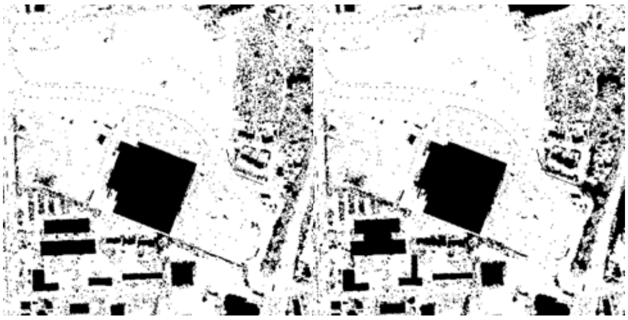

(c) nDSM , h=10 (d) nDSM , h=15

Figure 5. Different nDSMs based on grayscale reconstruction

Using now a complete sequence of marker images gives the chance to find the proper height offset level – say the discontinuity level - at which each of the off-terrain regions shows up individually with maximum height discontinuity along its boundary. In this way off-terrain regions with a variety of different sizes and heights are extracted.

5. EXPERIMENTS AND DISCUSSION

The concept for separating terrain from off-terrain points is tested with a LIDAR data set which shows a suburban area (Figure 6). The data have been recorded with TopScan's Laser Terrain Mapper systems, (TopScan, 2005). A regularly spaced elevation grid is generated by means of nearest neighbor interpolation of the raw 3D points.
The data sets are recorded in a district called Ickern of the city of Castrop-Rauxel, which is located in the west of Germany. The average density of the irregularly recorded 3D points is close to one per square meter; a one meter lattice spacing is chosen the elevation grid.

Buildings of different height and extend and 3D vegetation, which was not fully penetrated by the last pulse Laser beams, can be easily recognized. Also roads, bridges and even some field structures can be seen in Figure 6

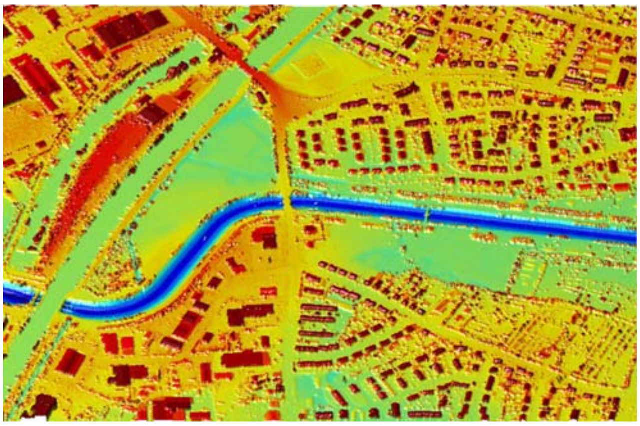

Figure 6. Last pulse range image – Ickern, Germany

The procedure for separating terrain and off-terrain points is now applied to the last pulse elevation grid. The surface model generated from the LIDAR data after removing all off-terrain points, i.e. a DTM, is visualized in Figure 7 using the same color table. .

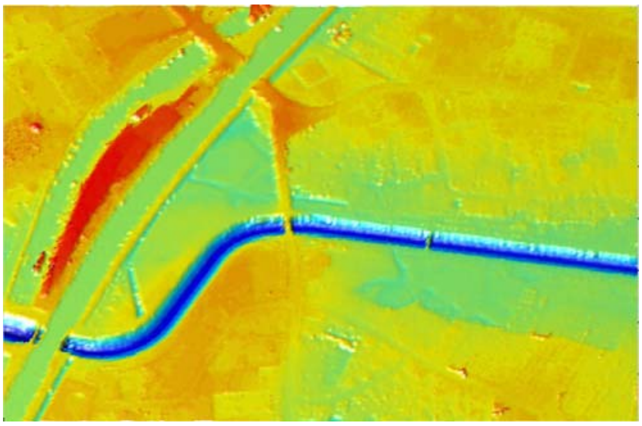

Figure 7. DTM generated with the morphological reconstruction algorithm (all off terrain pints have been eliminated

Figure 7 and in more detail Figure 8 show that almost all the eye-catching off-terrain regions have been eliminated. These regions mainly represent buildings and vegetation areas. None of the buildings is visible any more and also the vegetation has virtually disappeared. Interestingly, the bridges are preserved except one (the red colored one in the upper-left region of the test area).

Shape and size of the objects is obviously irrelevant in our approach. Large buildings as well as small ones, elongated buildings as well as shortened ones and high buildings as well as low ones have been properly eliminated.

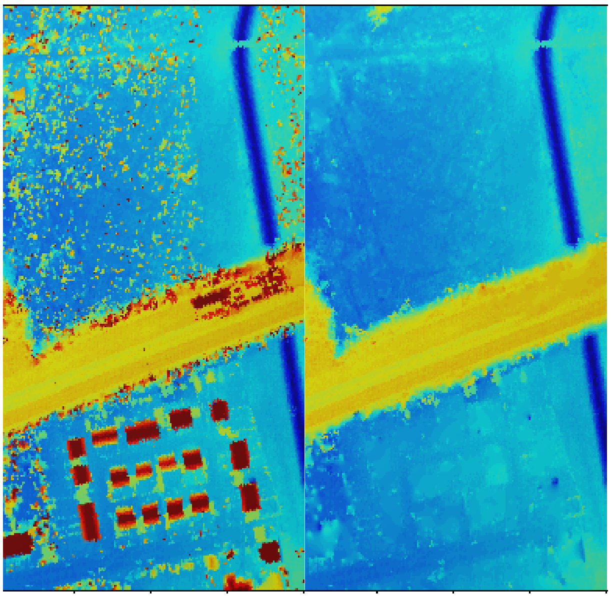

Figure 8. Mored detailled view of input elevation data (left) and the processing result visualsid by the DTM (right)

6. SUMMARY

In this paper an approach is presented to separate off-terrain points from terrain points in laser scanning data. Basis of the approach is a morphological reconstruction process which employs geodesic dilation. A significant advantage of geodesic filtering is that dilation uses an elementary isotropic kernel thus there is no need to specify kernel sizes like in other morphological approaches.
By running the geodesic dilation over a sequence of marker images off-terrain objects of varying height are taken into account. Within the sequential processing a classification is carried out to separate off-terrain and terrain regions. The off-terrain regions are further analyzed by investigating the local height difference along the boundary of the objects. This corresponds to analyzing the discontinuity by taking the slope along the boundary of the objects into account.

The first experiments demonstrate the efficiency of the approach and its capacity to separate terrain from non-terrain LIDAR points. Visually the procedure is already working quite well. Regardless of shape, extend and height of objects like buildings the LIDAR points have been successfully eliminated. Currently ground truth data are collected using aerial images to have a proper reference for more detailed investigations of the efficiency and quality of the process.
Future work may also focus on the classification process. Conceptually the process is prepared to extract and use many features for the classification of the off-terrain regions.

7. REFERENCES

Ameri B., "Automatic Recognition and 3D Reconstruction of Buildings from Digital Imagery", PhD Thesis, Institute of Photogrammetry, Stuttgart University, DGK-C 526, 2000

Arefi H., Hahn M., “A hierarchical procedure for segmentation and classification of airborne LIDAR images”, IGARSS symposum 2005, in press

Axelsson, P., "Processing of laser scanner data algorithms and applications". ISPRS Journal of Photogrammetry and Remote Sensing, 54, 1999, pp. 138 -147.

Jähne B., Haußecker B., Geißler P., 1999: Handbook of Computer Vision and Application, Volume II, Signal Processing and Pattern Recognition, Academic Press

Kilian J., Haala N., Englich M., “Capture and evaluation of airborne laser scanner data,” International Archives of Photogrammetry and Remote Sensing, Vol. XXXI, B3, Vienna, Austria, 1996.

Kraus K., Pfeifer N., “Determination of terrain models in wooded areas with airborne laser scanner data”, ISPRS Journal of Photogrammetry and Remote Sensing, 53, 1998, pp. 193-203.

Lantuejoul Ch, Maisonneuve F., “Geodesic methods in image analysis”, Pattern recognition, vol. 17, pp.117-187, 1984

TerraScan, URL: http://www.terrasolid.fi/ENG/ Tuote_kuvaukset /TScan .htm, Terrasolid Ltd, visited on May 2005

TopScan, URL: http://www.topscan.de/, visited on March 2005

Vincent L., “Morphological Grayscale Reconstruction in Image Analysis: Applications and Efficient Algorithms”, IEEE Transactions on Image Processing, Vol. 2, No. 2, pp. 176-201, April 1993.

Vosselman G., “Slope based filtering of laser altimetry data”. IAPRS, Vol XXXIII, Part B3, Amsterdam, The Netherlands. pp. 935-942, 2000

Wack R., Wimmer A., 2002: “Digital Terrain Models From Airborne Laser Scanner Data – A Grid Based Approach”. IAPRS, Vol XXXIV Part 3B. ISPRS Commission III, Symposium. September 9 - 13, 2002, Graz, Austria. pp. 293- 296.

Weidner U.: Digital Surface Models for Building Extraction, in: A. Grün (Ed.): Automatic Extraction of Man-Made Objects from Aerial and Space Images (II), 1997

Zhang K, Chen S, Whitman D, Shyu M, Yan J, and Zhang C, "A Progressive Morphological Filter for Removing Non-Ground Measurements from Airborne LIDAR Data," IEEE Trans. on Geoscience and Remote Sensing, Vol. 41, Issue 4, pp. 872-882, April 2003.